Lund University GEM thesis series nr 17

Improvement of the GPP estimations for Sudan using the evaporative fraction as water stress factor

Maria Angela Dissegna

2016
Department of Physical Geography and Ecosystem Science
Lund University
Sölvegatan 12
S-223 62 Lund
Sweden

LUND UNIVERSITY

UNIVERSITY OF TWENTE.
ITC
FACULTY OF GEO-INFORMATION SCIENCE AND EARTH OBSERVATION

Improvement of the GPP estimations for Sudan using the evaporative fraction as water stress factor

by

Maria Angela Dissegna

Thesis submitted to the department of Physical Geography and Ecosystem Science, Lund University, in partial fulfilment of the requirements for the degree of Master of Science in Geo-information Science and Earth Observation for Environmental Modelling and Management

Thesis assessment Board

First Supervisor: Jonas Ardö, Department of Physical Geography and Ecosystem Science (Lund University)

Examiner 1: Karin Hall, Department of Physical Geography and Ecosystem Science

Exam committee: Dan Metcalfe, Department of Physical Geography and Ecosystem Science

Disclaimer

This document describes work undertaken as part of a program of study at the University of Lund. All views and opinions expressed therein remain the sole responsibility of the author, and do not necessarily represent those of the institute.

Course title: Geo-information Science and Earth Observation for Environmental Modelling and Management (GEM)

Level: Master of Science (MSc)

Course duration: January 2016 until June 2016

Consortium partners:

The GEM master program is a cooperation of departments at 5 different universities:
University of Twente, ITC (The Netherlands)
University of Lund (Sweden)
University of Southampton (UK)
University of Warsaw (Poland)
University of Iceland (Iceland)

Abstract

The Gross Primary Production GPP quantifies the amount of carbon entering an ecosystem. It is an ecosystem service since it is a source of energy for all organisms and it is estimated to reduce atmospheric CO2 in about 123 Pg C per year at the global scale. Therefore, the improvement of estimation methods at large spatial scales using tools such as remote sensing has gain relevance in the last years.

The study evaluates two approaches of a Light Use Efficiency model with the aim to improve existing estimations of GPP in semi-arid areas. The tested inputs were the Fraction of Absorbed Photosynthetically Active Radiation (FAPAR) and the Enhanced Vegetation Index (EVI) used to represent the existent vegetation; coupled with the Evaporative Fraction as a term to represent moisture availability. The two approaches were tested trough a site level comparison between the GPP estimated from the records of the Eddy covariance flux tower located in Demokeya site in Sudan and the MODIS GPP product MOD17A2.

The results show that the inclusion of the Evaporative Fraction increased the accuracy of the GPP estimations in the two approaches during the dry seasons but it underestimates of GPP during the rainy seasons. Both approaches performed significantly better compared to the existing MODIS GPP estimations (MOD17A2) and overall the use of FAPAR performed better than EVI for the case of Demokeya site.

Keywords: Gross primary production, evaporative fraction, Light use efficiency models, semi arid regions.

Link to final presentation: https://prezi.com/gthfuyimvbkd/gpp/

Table of contents

Introduction

Global estimation and monitoring of plant photosynthesis known as Gross Primary Production (GPP) is an important component of climate change research. GPP flux determines the quantity of carbon entering an ecosystem. The study of GPP at larger spatial and longer time scales is necessary to identify locations of potential sinks or sources of carbon(Kanniah et al., 2010) and contributes to our knowledge on vegetation dynamics and responses to perturbations due to increased CO2 levels and changing environmental conditions. Estimates are highly uncertain and there is more information required to fully understand the temporal and spatial dynamics of ecosystems productivity across the world (Sjöström et al., 2011).
Africa has a recognized role in the global carbon cycle as it faces particular changes with respect to climate change and human pressure in all the different ecosystems (Hulme et al., 2001). Understanding the relationship between rangeland production and to water availability is of interest for the implementation of monitoring systems to support policies to reduce the socio-economic impacts of environmental stresses (Nutini et al., 2014). Improving the quantification of the atmospheric carbon exchange across the different vegetation types provides fundamental information that can be used to evaluate the performance of current terrestrial carbon cycle models (Merbold et al., 2008).

The main parameters affecting the variability of the GPP estimates in semi arid areas are water stress, radiation, fire, precipitation, vegetation composition, % vegetation cover and vegetation type. Since water availability is the main limiting factor for vegetation production in drier areas such as Sudan, especially where average annual rainfall is lower than 500/600 mm (Hein et al., 2011), the interest to estimate rainfall and soil moisture at the regional scale in relation to biomass production has earned a lot of attention (Nutini et al., 2014).
The use of remote sensing facilitates the quantification and monitoring of the ecosystem carbon uptake via photosynthesis over large geographic extents and periodic time scales. It relies on the robust relationship between satellite estimated light interception and photosynthesis through the use of Light Use Efficiency models (LUE) (Monteith, 1972) and their comparison to in situ measurements provided by flux towers (Krofcheck et al., 2015).
One of the primary sources of remote sensing based GPP estimates at the global scale is the MODIS product MOD17 (Running et al., 2004). It has some limitations coming from the use of coarse resolution meteorological data (Heinsch et al., 2006; Zhao et al., 2006) and the dependency on estimates of LUE taken from vegetation type look up tables that may contain errors in either the original estimates of maximum LUE for a particular vegetation type or when designating the vegetation types.

Aim of the study

This study employs a combination of remote sensing products and the inclusion of the evaporative fraction (EF) as limiting factor of a light use efficiency model (LUE) estimating GPP.

The aim of this study is to evaluate two approaches to improve the existing estimation of GPP (ex. MOD17A2) in semi-arid areas; one using as input the Fraction of Absorbed Photosynthetically Active Radiation (FAPAR) and the second using the Enhanced Vegetation Index (EVI). The study period is from 01/May/2007 to 31/Dec/2009, allowing a site level comparison between the GPP estimated from Eddy covariance flux tower records from the Demokeya site in Sudan and the MODIS GPP product MOD17A2.

Hypothesis

The hypothesis is that the use of the evaporative fraction in a LUE model will derive more accurate estimates of GPP than the MODIS MOD17A2 product; such estimates being closer to the real GPP (estimated from Eddy covariance flux tower).
H_1: The inclusion of the evaporative fraction as a limiting factor of a LUE model derives more accurate estimates compared to the GPP measurements from the flux tower and MOD17A2 MODIS GPP product.
H_0: There is no significant evidence of an improvement in the estimations when including EF.

Background

Primary production is the rate of biomass accumulation. GPP is the total amount of carbon produced by vegetation used for growth and maintenance and is an important variable defined as the overall photo-synthetic fixation of carbon per unit space and time (i.e. g C m^{-2} $year^{-1}$). Net primary production represents the total available energy in an ecosystem as dry biomass (Abdi et al., 2014). Therefore, NPP is the annual sum of GPP minus the autotrophic respiration which is the energy used for maintenance.
The study of GPP provides important information about the environment, as vegetation is a critical component of the global carbon cycle mainly due to photosynthesis, which regulates the flux of carbon between the biosphere and atmosphere. GPP is also important ecosystem service since it is estimated to reduce atmospheric CO_2 in around 123 Pg per year at a global scale (Beer et al., 2010). The study of carbon flux variation over time provide useful knowledge regarding possible factors influencing the carbon cycle and to make future estimates (Stagakis et al., 2007).
Satellite remote sensing can provide consistent observations of land surface properties over large areas and has become an important input for GPP estimates (Wang & Mo, 2015). A number of remote sensing based GPP models have been proposed and widely used for GPP simulation at different scales, among which the temperature and greenness (TG), greenness and radiation (GR) and vegetation photosynthesis model (VPM) are characterized by the advantages of fewer parameters and high accuracy. The GR model applies remote estimation of chlorophyll content for retrieval of the GPP, which provides a robust estimation of midday GPP (Gitelson et al., 2006). The TG model combines EVI and LST and improves the correlation between the estimated and observed data. It performed well predicting GPP for several evergreen needle leaf and deciduous broadleaf forests in North America (Sims et al., 2008).

Kanniah et al., (2009)showed accurate estimates of input parameters such as photosynthetic active radiation (PAR), fraction of absorbed PAR (FAPAR), LUE, vapor pressure deficit (VPD) and minimum temperature (TMIN) scalars can produce reliable estimate of GPP even with a simple LUE model for single savanna sites in northern Australia.

The eddy covariance (EC) technique provides net CO2 exchange estimates at high temporal resolution, which can be used for developing and validating GPP models (Wang & Mo, 2015). Unfortunately the number of stations is limited spatially, being about 16 stations across the African continent ("European Fluxes Database Cluster - Sites List," n.d.).
Studies such as (Ma et al., 2014) seek to find an appropriate method to accurately up-scale savanna GPP from local measurements from EC flux tower data to regional scales utilizing remote sensing observations. They assessed the seasonal patterns of remote sensing products versus the seasonal EC tower GPP for four sites along an ecological rainfall gradient, where tropical wet and dry savannas are found. They concluded that EVI tracked the seasonal variations of GPP (EC flux tower) well at both site- and cross-site levels (R^2= 0.84). Additionally, the coupling of an ecosystem light-use-efficiency model (eLUE) strengthened the EVI - GPP EC flux tower relationship.

Although the previously mentioned models performed well in terms of vegetation in specific areas, they have substantial variations and uncertainties and should be further readapted for different climatic regions. The seasonal variability of carbon uptake depends on structural and physiological constraints of the ecosystem functions such as moisture, temperature, nutrient availability, atmospheric CO_2 concentrations and mix of plant functional types. Estimations of the seasonality of vegetation from leaf area or other parameters such as FAPAR or EVI depends on coupling the absorbed radiation seasonality and the efficiency of photosynthetic light use to the environmental constraints on plant growth (Bondeau, et al., 1999).

In semi-arid regions as Sudan, vegetation function is constrained by water availability throughout the year, with periods of drought and heat followed by pulses of precipitation in the rainy season (Krofcheck et al., 2015). In biomes such as savanna, the parameterization of plant functioning is especially difficult due to the presence of varying mixtures of multiple plant functional types (i.e. trees and grasses) with distinct responses to environmental factors and different phenologies (Ma et al., 2014).

To address this problem instead of using a simple LUE model, Ma et al, (2014) used an eLUE model which is a ratio of GPP against incoming photosynthetically active radiation (PAR). The model investigaes the top-of-canopy incident PAR (PARTOC) and top-of-atmosphere incident PAR (PARTOA). Some of the advantages of the eLUE were the reduction of the seasonal hysteresis observed between the growing season and the drying season in GPP-EC and MODIS satellite product relationships, resulting in a consistent estimation of GPP across phenophases.

The eLUE model simplified the up-scaling of carbon fluxes from tower to regional scale, effectively integrating the effects of variations in canopy photosynthetic capacity and environmental stress on photosynthesis.

The results from the study demonstrated that savanna GPP can be accurately estimated at regional scale entirely with remote sensing observations without dependency on ground meteorological data or the estimation of LUE parameters.

Environmental stress related to temperature and water availability has shown to modify the light use efficiency at short time scales such as hours to days. (Russell et al., 1989). One of the main responses to leaf stress is the increase in the visible reflectance. This happens due to a combination of stressors which reduce the chloropyll a + b content leading to a reduction in the absorption of incident light (Carter & Knapp, 2001; Hendry et al., 1987).

The Evaporative Fraction (EF) can represent moisture availability for plants. It is the ratio of the energy exported as evaporated water as latent heat (LE) to the LE and sensible heat (H). A lower EF is generally a characteristic of ecosystems with sparse vegetation cover and dry conditions (Li et al., 2006). Several studies have previously used EF as an indicator of water availability in ecosystems since it is strongly influenced by the soil moisture at the rooting-zone, which is the main limiting factor influencing latent heat flux (Kurc & Small, 2004).
EF can be calculated from the EC data of water vapor and heat transfer, and from remote sensing products using the albedo-land surface temperature (LST) relationship (Nutini et al., 2014).

Study area

The study area is the country of Sudan (Figure 1), the climate ranges from arid in the north to tropical wet-and-dry in the far southwest. Temperatures are the highest at the end of the dry season, when cloudless skies and dry air allow them to rise. In average 41°C with a maximum reported of 49°C. The far south, however, with only a short dry season, has uniformly high temperatures throughout the year(Metz, 1991).

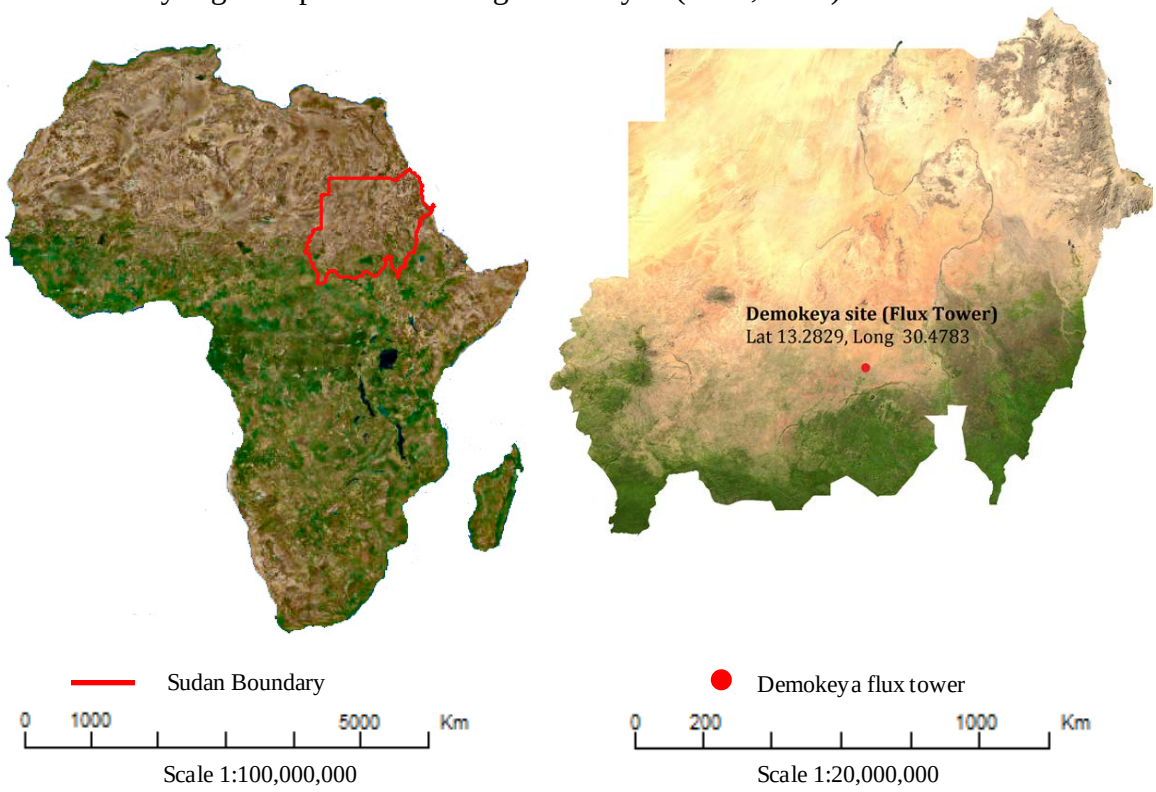

Figure 1. Location of Sudan and Demokeya site.

The most significant climatic variables are rainfall and the length of the dry season. The country's territory falls between the 100mm isohyets in the north and 800 mm isohyets in the southernmost areas (Ardö, 2013). Variations in the length of the dry season depend on which of two air flows predominates dry northeasterly winds from the Arabian Peninsula or moist southwesterly winds from the Congo River basin (Metz, 1991). Sudan has one yearly rainy season, with majority of rainfall occurring in late July to October, initiating germination of annual species and the growing season onset. In some years the arrival of rain in central Sudan can be delayed or may not come at all. When that happens, drought and famine follow as it happened the decades of the 1970s and 1980s with disastrous results for the Sudanese people and economy (Metz, 1991).
The country's soil types are wide and diverse, with sandy soils found in the northern and west central areas, clay in the central regions and lateritic in the south. Alluvial soils are found along the lower reaches of the rivers and deltas. The most important soils for

agriculture are the clays in central Sudan that extend from west of Kassala through Al Awsat and southern Kordofan. The East of the Blue Nile is used for mechanized rain fed crops. To the west of the White Nile soils are used to grow sorghum, sesame, peanuts, and cotton as traditional agriculture. The southern part of the clay soil zone lies in the broad floodplain of the upper reaches of the White Nile and its tributaries are subject to heavy rainfall during the rainy season. The floodplain is then inundated for four to six months and adjacent areas are flooded for one or two months. Overall, this area is poorly suited to crop production, but the grasses during dry periods are used for grazing. Sandy soils in the semiarid areas south of the desert in northern Kordofan and northern Darfur states support vegetation also used for grazing. Livestock rising is this area's major activity, but a significant amount of crop cultivation, mainly of millet, also occurs. Peanuts and sesame are grown as cash crops. The laterite soils of the south cover most of western Al Istiwai and Bahr al Ghazal states. Those underlie the extensive moist woodlands found in these provinces. Crop production is scattered, and the soils when cultivated lose fertility relatively quickly; even the richer soils are usually returned to bush fallow within five years (Metz, 1991).

The Sahelian landscape and semiarid region is composed with sparse savannah and millet fields, grasslands and open woody savanna. The herbaceous layer is dominated by annual and perennial grasses including the annuals *Eragrostis tremula, Cenchrus biflorus* and some herbs, and the perennial *Aristida pallida*. In Demokeya site, the dominating woody species are of the *Acacia genus*, including *Acacia nilotica, Acacia tortilis,* and *Acacia Senegal* and constitute 5%–10% of canopy cover (Ardö, 2013).

Methodology and materials

GPP estimation through light use efficiency model (LUE)

The LUE model stems from linear relationship that exists between the amount of photosynthetic active radiation (PAR) absorbed by vegetated canopies (APAR), and their net or gross primary productivity (Monteith, 1972). It represents the efficiency with which plants use solar energy to assimilate carbon. LUE differs across biomes, plant functional types, stages of succession, and species (Gower, Kucharik, & Norman, 1999), and is also temporally dynamic in response to environmental variations(Landsberg & Waring, 1997);(Nouvellon et al., 2000); (Turner et al., 2003).
A conversion efficiency term (ε) is used in the relationship, such that:

$$GPP = \varepsilon * APAR$$
$$GPP = \varepsilon * PAR * fAPAR$$
$$GPP = \varepsilon max * (EF) * PAR * fAPAR \quad (1)$$

Where:

GPP is the gross primary production (g C $m^{-2}day^{-1}$),
PAR is the photosynthetic active radiation incident on the canopy (MJ $m^{-2}d^{-1}$),
fAPAR is the fraction of incident PAR that is absorbed by the canopy,
ε is the light use conversion efficiency (LUE) of the vegetation (g C MJ^{-1}) and is the amount of carbon a specific vegetation type can produce per unit of energy and is calculated as:

$$\varepsilon = \varepsilon max * (EF) \quad (2)$$

Where:
ε max is the biome-specific maximum conversion efficiency (g C MJ^{-1}) the used values are according to the study by (Garbulsky et al., 2010),
EF is the evaporative fraction, used as a water availability multiplier that reduces the conversion efficiency when water availability becomes a limit for the plant function. EF is a measure of the portion of the available energy used for evapotranspiration and is calculated according to (Nutini et al., 2014) methodology. *EF* can range from 0 (total inhibition) to 1 (no inhibition).

$$EF = \frac{\lambda E}{\lambda E + H} \quad (3)$$

Where:
λE is the latent heat [W m^{-2}], which is the amount of energy released or absorbed by water during a change of state.
H is the sensible heat flux [W m^{-2}], both of which are measured at the EC towers and can be calculated from remote sensing (Nutini et al., 2014).

A variation to the approach would be the use of EVI as a proxy for FPAR.

GPP can be estimated through a linear regression model with relatively high accuracy using only EVI as independent variable (Sjöström et al., 2008). They showed that EVI had the highest correlation among the three vegetation indices studied (EVI, the Normalized Difference Vegetation Index NDVI and the Shortwave Infrared Water Stress Index SIWSI) for an agricultural site and a semi-arid savanna shrub site. Their results suggests that EVI shows significant promise for efficient determination of primary production, and that a simple modeling approach, based solely on EVI, can be utilized to give reliable estimates of GPP at similar ecosystems.
Considering EVI = fAPAR (Garbulsky, Peñuelas, Papale, & Filella, 2008) then,

$$GPP = PAR * EVI * \varepsilon max * EF \quad (4)$$

where:

$$EVI = G * \frac{R_{Nir} - R_{Red}}{L + R_{Nir} + C_1 * R_{Red} - C_2 * R_{Blue}} \quad (5)$$

R_{Red}, R_{NIR} and R_{Blue} are the spectral reflectances in MODIS bands 1, 2 and 3 respectively.
G, L, C1 and **C2** are constants with values of **2.5, 1, 6.0** and **7.5** respectively.

To be calculated from the 8-day MODIS surface reflectance data [MOD09A1 band 1 (620– 670 nm), band 2 (841–876nm), band 3 (459–479 nm)]

Another possible approach would be to use a temperature greenness model which combines EVI with land surface temperature (Sims et al., 2008). LST has shown to be closely related to the vapor pressure deficit (VPD) (Granger, 2000) and therefore may provide a measure of drought stress. The LST product from MODIS can be used both as a measure of temperature and VPD (Hashimoto et al., 2008). There is also a MSG/SEVIRI based LST product (Peres, 2005).
The main limitations of the simple model are the lack of estimates of the timing of the photosynthetic active period for sites with evergreen vegetation and the poor estimations of GPP for active season in sites that present summer droughts or with predominant evergreen vegetation(Sims et al., 2008).
By including LST in addition to EVI, the TG model avoids many of the limitations of the simple model that uses EVI alone. Since the inactive periods were mostly the result of summer drought characterized by high temperatures and VPD, it is clear that the inclusion of a measure of temperature and drought stress could improve the model (Sims et al., 2008).

$$GPP = PAR * EVI * \varepsilon max * VPD*(T) \quad (6)$$

The LST method for predicting VPD for global and regional scales was revisited by Hashimoto et al., (2008) concluding that it overestimates VPD in areas within 50 km of coastlines and underestimates VPD in very arid and non-vegetated regions. The uncertainty increases when higher values of VPD are reported and cloud contamination limits the near real-time ecological monitoring. The advantage is that the VPD method

can be easily implemented and satellite observations can be translated to estimates of evapotranspiration by using ecosystem models, preferably, with the correction of biases using ground-observation data (Hashimoto et al., 2008). This approach was not included in the final results.

PAR

Photosynthetic active radiation corresponds to the spectral range of solar radiation from 400 to 700 nanometers that photosynthetic organisms are able to use in the process of photosynthesis (McCree, 1981). The data used for PAR comes from the Meteosat Second Generation (MSG) Surface incoming shortwave radiation (SIS) and is the radiation flux density reaching a horizontal unit earth surface in the 0.2-4 μm wavelength range. It is usually also called global irradiance or solar surface irradiance. It is expressed in W m-2. The product comes from the MSG Spinning Enhanced Visible and Infrared Imager (SEVIRI) sensor which is in geostationary orbit over Africa and collects data every 15 minutes, which can then be integrated for longer time spans (Aminou, 2002). Some limitations of the SIS product for desert regions are the high clear sky reflection over bright surfaces which reduce the contrast between clear sky reflection and cloudy-sky reflection leading to higher uncertainties in effective cloud albedo and errors in the calculation of SIS (Acker et al., 2010). The accuracy of aerosol information is not well defined in several regions of the world due to missing ground measurements. Uncertainties in the aerosol information affects SIS accuracy, especially in predominantly clear sky regions (Acker et al., 2010)

FAPAR

FAPAR is the fraction of photosynthetically active radiation absorbed by the canopy. FAPAR results directly from the radiative transfer model in the canopy which is computed instantaneously (Baret et al., 2006). It depends on canopy structure, vegetation element optical properties and illumination conditions. FAPAR is widely used as input for primary productivity models based on simple efficiency considerations (Prince, 1991).
FAPAR is an important environmental variable that can be used as indicator of the state and development of the vegetation cover (Gobron & Verstraete, 2009). The algorithm that derives the FAPAR compares the observed canopy reflectance against modeled radiance for a suite of canopy structures and soil patterns using biome specific lookup tables (Myneni et al., 1999).

APAR

APAR is the absorbed photosynthetic active radiation and is the product of FAPAR*PAR.

EVI

Major factors influencing empirical estimates of FAPAR using spectral vegetation indices are the leaf area index (LAI), vegetation spectral properties, pixel heterogeneity, background reflectance, solar zenith and view zenith angle, vegetation shadow fractions, atmospheric scattering and bidirectional reflectance effects (X. Li & Strahler, 1985); (Myneni & Williams, 1994). Some of these factors can be mitigated using advanced indexing techniques such as the enhanced vegetation index.
Vegetation indexes are robust and seamless biophysical measures, which are computed in the same way across all pixels of a group of satellite images regardless of land cover condition, soil type or biome (Huete & Glenn, 2011). The enhanced vegetation index is widely used as a proxy of canopy greenness and chlorophyll content (Myneni & Williams, 1994).
The computation of EVI quantifies the difference in visible red light reflection in situations where absorption is dominated by green leaves. It also quantifies the near infrared (NIR) wavelengths where light scattering is dominated by cell walls (Tucker, 1979) ,thus, giving information about variations of vegetation in time and space while enhancing the vegetation signal by reducing the influences from the atmosphere and canopy background and to improve sensitivity in high biomass regions (Huete, Liu, Batchily, & Van Leeuwen, 1997);(Huete et al., 2002). EVI is estimated from surface reflectance in the red and NIR bands but it also uses reflectance in the blue band to correct for effects of aerosols. Using surface reflectance data from MODIS MOD09A1 product, EVI is calculated as:

$$EVI = 2.5 * \frac{R_{Nir} - R_{Red}}{1 + R_{Nir} + 6 * R_{Red} - 7.5 * R_{Blue}} \quad (7)$$

Light conversion efficiency and maximum conversion efficiency (ε max)

Vegetation type is assumed to be the main control of light use efficiency at the annual scale, but large variability among LUE occur within each vegetation type (Ruimy, et al., 1994; Gower et al., 1999). Drivers of spatial and temporal variability of LUE are forest age, management practices and nutritional status (Mäkelä et al., 2007;Ollinger et al., 2008). The maximum LUE is set as a constant and is subsequently downregulated by temperature and estimators of water stress in models that estimate GPP (Potter et al., 1999;Running et al., 2004;Yuan et al., 2007; Mäkelä et al., 2007). There are different strategies to define the maximum LUE values and each of the coefficients that account for the stress effects are used to estimate the actual LUE. Garbulsky et al., (2008) defined the maximum LUE (gC MJ APAR-1) from each FAPAR estimator and site type, as the maximum gross LUE that is attained by vegetation for the duration of the analysed growing seasons.

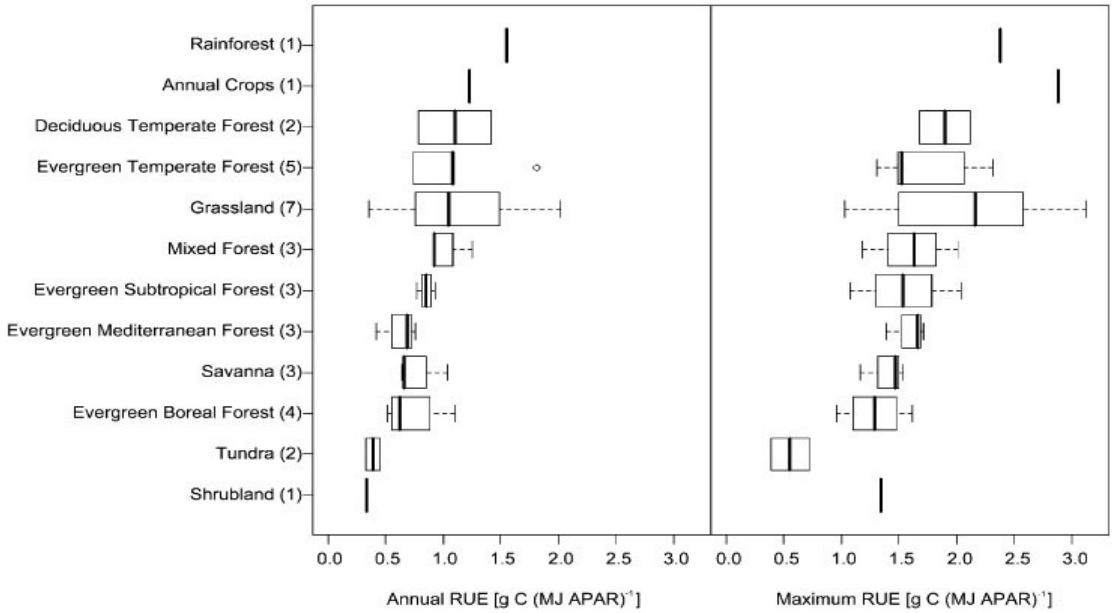

Figure 2. Variability of LUE copied from (Garbulsky et al., 2010).

In this study εmax was assigned to the different land cover classes based on the values found in (Garbulsky et al., 2010). The maximal LUE for each land cover type is used. Different LUE max values have been used in the literature and (Figure 2) shows the variability of LUE according to a study by Garbulsky et al., (2010). (Table 1) shows the five LUE max values tested for the calculation of the 1x1 Km area surrounding the flux tower. The LUE max for grassland (2.2 g C MJ^{-1} $APAR^{-1}$) provided the closest results to the estimations from the tower. (Table 2) Shows the final LUE max values assigned to each land cover type used for the GPP calculations for the territory of Sudan. The table also compares the values suggested by (Garbulsky et al., 2010) and the LUE max used for the calculations of the MOD17A2 GPP product(Running & Zhao, 2015)

Table 1. LUEmax values tested for calculations in the subset area

	Cover type	LUEmax g C MJ^{-1} $APAR^{-1}$
1	Grassland (Garbulsky)	2.2
2	Grassland (BPLUT MOD17)	0.86
3	Savanna(Garbulsky)	1.5
4	Woody savanna (BPLUT MOD17)	1.239
5	Savanna (BPLUT MOD17)	1.206

Table 2. LUE max values.

Class	UMD classification	Garbulsky LUEmax g C MJ^{-1} $APAR^{-1}$		MOD17 LUEmax g C MJ^{-1} $APAR^{-1}$	
0	Water	Water	0	Water	0
1	Evergreen Needleleaf forest	Evergreen Boreal forest	1.35	ENF	0.962
2	Evergreen Broadleaf forest	Evergreen Subtropical	1.6	EBF	1.268
3	Deciduous Needleleaf forest	/	1.3*	DNF	1.086
4	Deciduous Broadleaf forest	Decidious temperate forest	1.3	DBF	1.165
5	Mixed forest	Mixed forest	1.65	MF	1.051
6	Closed shrublands	Shrubland	1.4	CS	1.281
7	Open shrublands	/	0.9*	OS	0.841
8	Woody savannas	/	1.55*	WS	1.239
9	Savannas	Savannas	1.5	S	1.206
10	Grasslands	Grasslands	2.2	G	0.86
12	Croplands	Annual crops	2.9	C	1.044
13	Urban and built-up	x	0	U	0
16	Barren or sparsely vegetated	x	0	B	0
		rain forest	2.4	/	

Values marked with * where designated by me.

Estimation of Evaporative Fraction (EF)

The estimation of evaporative fraction was obtained using the albedo-temperature method using MODIS albedo and land surface temperature (LST) products. EF stems from the heat balance equation:

$$R_n = \lambda E + G_O + H \quad (8)$$

where:

R_n	is the net radiation arriving to the soil
λE	is the latent heat flux
λ	is the latent heat for the vaporization of water
E	is the evapotranspiration
G_o	is the heat flux spread under the soil surface
H	is the sensible heat flux

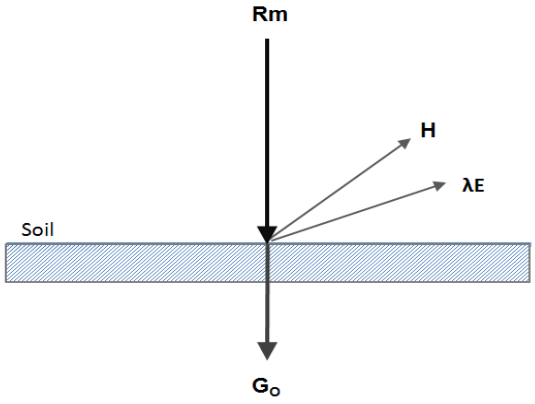

Figure 3. Soil heat balance

The evaporative fraction is the relationship between the latent heat flux and the total heat flux coming from the soil.

$$EF = \frac{\lambda E}{\lambda E + H} = \frac{\lambda E}{R_n - G_0} \quad (9)$$

The methodology to carry out in this part follows Nutini et al., (2014). In their approach, EF is calculated for every pixel as the relative distance from two lines, which are the dry edge and wet edge. These lines are defined through a date-specific albedo-LST relationship. In (figure 4), the blue circles correspond to minimum temperature values for each albedo class, which are used to calculate the wet edge (lower limit of the graph) through a linear regression. The red circles correspond to the maximum temperature values for each albedo class, which are used to calculate the dry edge (upper limit) through linear regression. TH (maximum temperature) and TλE (minimum temperature) represent the values used in the calculation of the EF for pixel i.

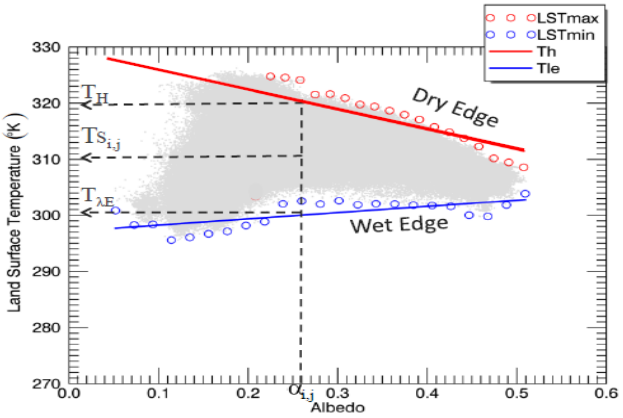

Figure 4. The scatterplot between surface albedo and LST is created for every image during the computation of EF (Nutini et al., 2014).

For the EF estimation, albedo and LST data were extracted from the digital numbers of MCD43B3 layer 10 and MOD11A2 layer 1. Information on LST data quality was obtained from Layer 2. Pixels flagged as no-data or low quality were excluded from the analysis.

To calculate EF, the albedo-LST scatterplot is derived for a single date and analyzed to extract minimum and maximum temperature values for all of the albedo classes.
The series of maximum and minimum LST values were used to calculate the date-specific dry and wet edge equation through linear regression:

$$\text{dry edge: } TH = m_{dry}\,\alpha 0 + q_{dry} \quad (10)$$
$$\text{wet edge: } T\lambda E = m_{wet}\,\alpha 0 + q_{wet} \quad (11)$$

where:

m and **q**	represent the slope and intercept of the two regression lines,
$\alpha 0$	represents the albedo,
T	is the land surface temperature [K].

The dry edge was defined considering only pixels with albedo value above 0.2 (Galleguillos et al., 2011).
Using the dry and wet edge, the EF is calculated for every pixel i, dividing the difference between TH and the temperature pixel TS by the difference between TH and TλE:

$$EF_i = \frac{T_{H\,i} - T_{s\,i}}{T_{H\,i} - T_{\lambda E\,i}} \quad (12)$$

where:

T_{si}	is the temperature value of the pixel *i*.
T_{Hi} and $T_{\lambda Ei}$	are respectively the maximum and minimum temperature value derived by the dry and wet edge functions for a given albedo value αi.

Therefore the EF equation can be rewritten as:

$$EF_i = \frac{(m_{dry}\,\alpha_i + q_{dry}) - T_{S\,i}}{(m_{dry}\,\alpha_i + q_{dry}) - (m_{wet}\,\alpha_i + q_{wet})} \quad (13)$$

The formula for the calculation of the EF was applied to each pixel of the4 MODIS tiles covering the territory of Sudan; and on each date available. It was implemented with an IDL code provided by dr. Nutini and dr. Candiani. EF maps where obtained and used for the GPP estimations. (Figure 5) shows the evaporative fraction in Sudan for the date with the highest EF value calculated for Demokeya site during the study period. Black regions correspond to no-data.

Evaporative fraction map for Sudan as September 3rd, 2008

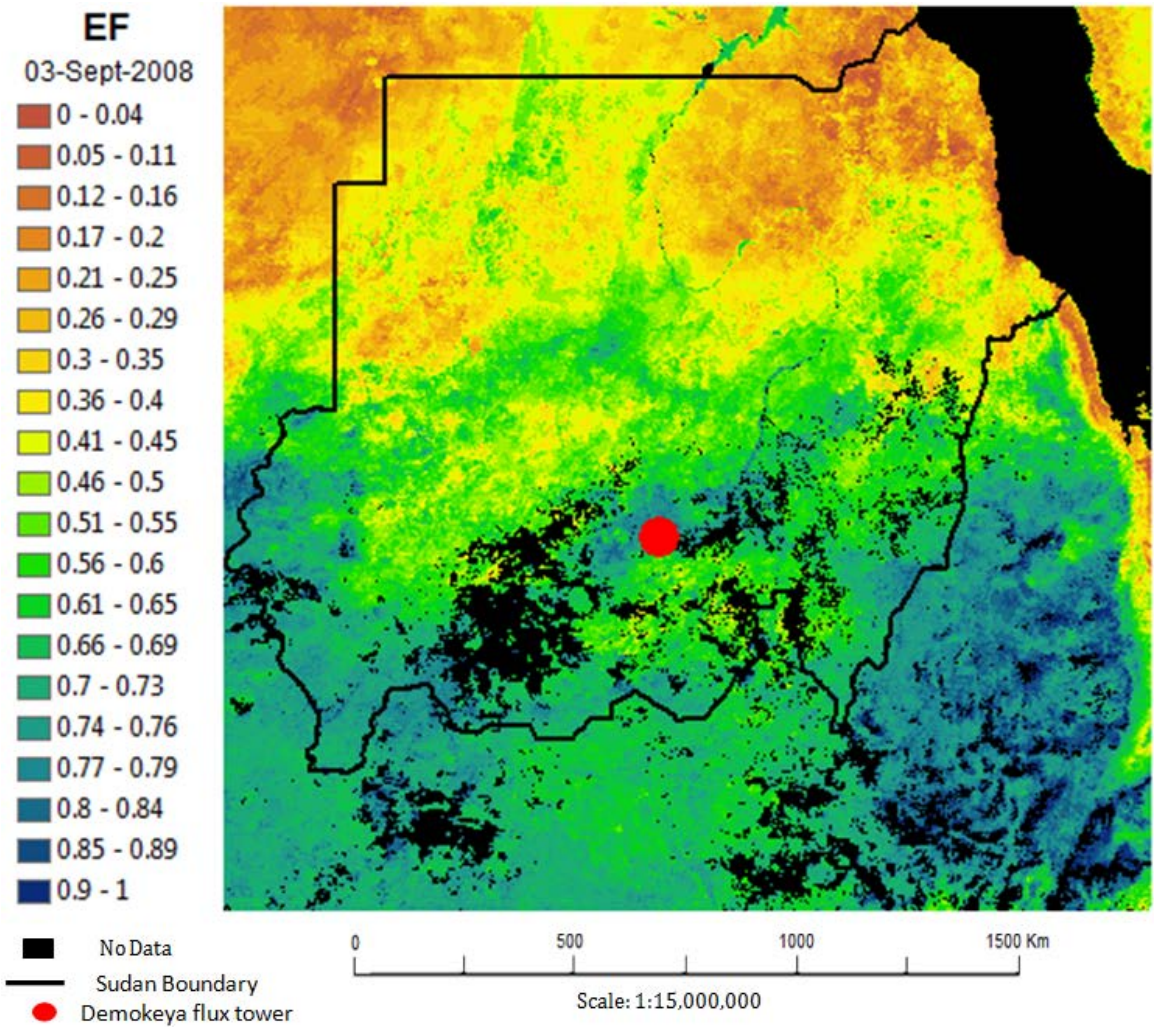

Figure 5. Evaporative fraction map for Sudan (September 3rd, 2008). Red colors denote very low EF while blue corresponds to high EF. This was the highest EF value at the Demokeya site in the studied period.

Data

To cover the country of Sudan, six MODIS tiles h20v06, h20v07, h20v08, h21v06, h21v07 and h21v08 obtained through the online Data Pool at the NASA Land Processes Distributed Active Archive Centre (LP DAAC), USGS/Earth Resources Observation and Science (EROS) Centre, Sioux Falls, South Dakota (https://lpdaac. usgs.gov/data_access) for the period 15/05 2007 to 31/12/2009, summing up to 492 images for each of the MODIS product used; and one MSG subset covering the territory of Sudan for each day of the study period. The characteristics of the data are summarized in the following products table.

Table 3. Data characteristics

Use	APAR estimation			controls on ε			Comparison
	PAR (Swrad *0.46)	FAPAR	EVI	Land cover	Evaporative Fraction (EF)		
Product	MSG SIS - Surface incoming shortwave	MOD15A2	MOD09A1	MCD12Q1	MOD11A2	MCD43B3	MOD17A2
Description	Daily Downward Surface Shortwave Flux	LAI/fAPAR	Surface reflectance	Land cover product	Land Surface Temperature/Emissivity	Albedo Band shortwave (Black	GPP
Level/collection	-	L4 v6	L3 v6	L3 v5.1	L3 v6	L3 v5	L4 v6
Layer/band used	subdataset 0	1km Fpar, layer 1 QC 3 and 4	Surface Reflectance Layer 1, 2 ,3 QC 8	Land Cover Type 2 (UMD)layer 1 QC 7 and 11	LST_DAY, Layer 1 QC_Day, layer 2	Albedo, Layer 10	GPP, layer 1 QC 3
Temporal granularity	daily	8 -day	8- day composites	1 -year	8-day	8-day	8-day
Spatial resolution	15km	500 or 1km	500m	500m	1km	1km	500m
Units of measurement	MJ/m2/day	Unitless fraction of incoming radiation	W/m2/µm/sr	16 classes of land cover	Kelvin	Albedo, no units	KgC/m2
Data for study	3.3GB	5.7GB	72.2GB	2.06GB	6.7GB	28.2GB	5.7GB

The data for PAR comes from the MSG Surface incoming Shortwave (SIS) product; it has a spatial resolution of 3 km and is a daily average of the 15-minutes observations. For the current study PAR is calculated as 46% of the SIS. According to (Iqbal, 1983)areas of low values likely correspond to clouds and/or aerosols (Aminou, 2002).

The data for FAPAR comes from the MODIS sensor mounted on NASA's Terra and Aqua satellites. The product name is MOD15A2 and is an 8day composite at 1 km spatial resolution (Myneni et al., 1999).

The data for EVI comes from the product MOD09A1 which provides surface reflectance in 8-day composites at a 500 m resolution. The data was radiometrically calibrated and atmospherically corrected to yield a surface reflectance product. Each pixel contains the optimal observation during an 8-day period. The data has been gridded to separate geolocation from compositing. The optimal coverage, observation, absence of clouds or shadow thereof, aerosol loading and low view angle was considered (Vermote, 2011). EVI time series were seasonally adjusted by an adaptive Savitzky-Golay filtering method using the TIMESAT program package (Jönsson & Eklundh, 2002, 2004). TIMESAT fits a function to the upper envelope of the satellite time series data, filtering out negatively biased noise due to atmospheric effects.(Eklundh & Olsson, 2003),(Olofsson et al., 2008). The already processed data was obtained from Jonas Ardö (Ardö *et al*, 2016).

The MODIS land cover type product MCD12Q1 describes land cover properties derived from observations spanning a year's input of Terra and Aqua- MODIS data. The product contains five classification schemes; it is a yearly product at 500m resolution. The layer used in this study is land cover type 2 University of Maryland (UMD) scheme which

corresponds to the one used in the MOD17A2 algorithm (Fallis, 2013). The LUE max values are assigned to each of the land cover classes of this product (Table 2).
The Land Surface Temperature MOD11A2 is 8-day product composed from the daily 1Km LST product MOD11A1 and stored as the average values of clear-sky LSTs during an 8-day period. The unit for the DN values is Kelvin degrees and it needs to be multiplied by a scale factor of 0.02 (Wan, 2006).
The Albedo product MCD43B3 provides 1Km data describing directional hemispherical reflectance (black-sky albedo) at local solar noon. The albedo quantities are produced from the 16-day anisotropy models provided in MCD43B1 and represent averages of the underlying 500m values (Strahler & Muller, 1999).
The MODIS Gross Primary productivity MOD17A2H (Collection 6) is a cumulative 8-day composite of GPP, NPP and PSN with 500 meter pixel size. GPP is calculated daily using a LUE based model where the maximum conversion efficiency of absorbed light energy (ε max) is modified by scalars of high daily vapor pressure deficit and low daily minimum air temperature respectively. The algorithm uses 6-hourly National Center for Environmental Prediction- Department of Energy (NCEP-DOE) reanalysis II for daily Tair, VPD and PAR. GPP values are expressed as Kg C m^{-2}. The product contains a Quality Control layer (Running & Zhao, 2015). The DN values where extracted as a subset and multiplied for a Scaling factor of 0.0001 to be evaluated against the study results and the EC GPP.

GPP from Eddy covariance flux tower

GPP was estimated from the Net Ecosystem Exchange (NEE) fluxes measured at the EC tower with using a standardized partitioning method for all the sites as described by (Reichstein et al., 2005) and (Papale et al., 2006). GPP is calculated from NEE by adding RE (Rossini et al., 2012). Flux measurements were collected at the eddy covariance tower situated in Demokeya experimental forest outside El Obeid, Kordofan, Sudan, coord: (13.2829, 30.4783) (http://fluxnet.ornl.gov/site/724) Meteorological data and soil data have been collected at a site in the central Sudan since 2002. In addition to basic meteorological variables, soil properties (temperature, water content, and heat flux) and radiation (global, net and photosynthetic active radiation) were measured. The dataset has a temporal resolution of 30 minutes and provides general data for calibration and validation of ecosystem models and remote-sensing-based assessments, and it is relevant for studies of ecosystem properties and processes (Ardö, 2013).
This site presents the typical Sahelian landscape with sparse savannah and millet fields. It is characterized by a sparse Acacia savanna in the semiarid region of Sudan. It has a canopy cover of 5–10% and a ground cover composed mainly of grasses and some herbs. The maximum tree height is six meters and the major part of the tree canopy is located between three and five meters above the ground. Grasses and herbs reach a maximum height of one meter. Approximately 70% of the vegetation is assumed to be C4 plants and 30% is assumed to be C3 plants (Ardö, 2013).
The mean annual precipitation is 320 mm with most falling from June to October. The period from November to May is dry and the seasonality of the precipitation is strong.

Data process

The figure 6 illustrates the steps applied for each of the satellite products and the corresponding calculations for the entire study.

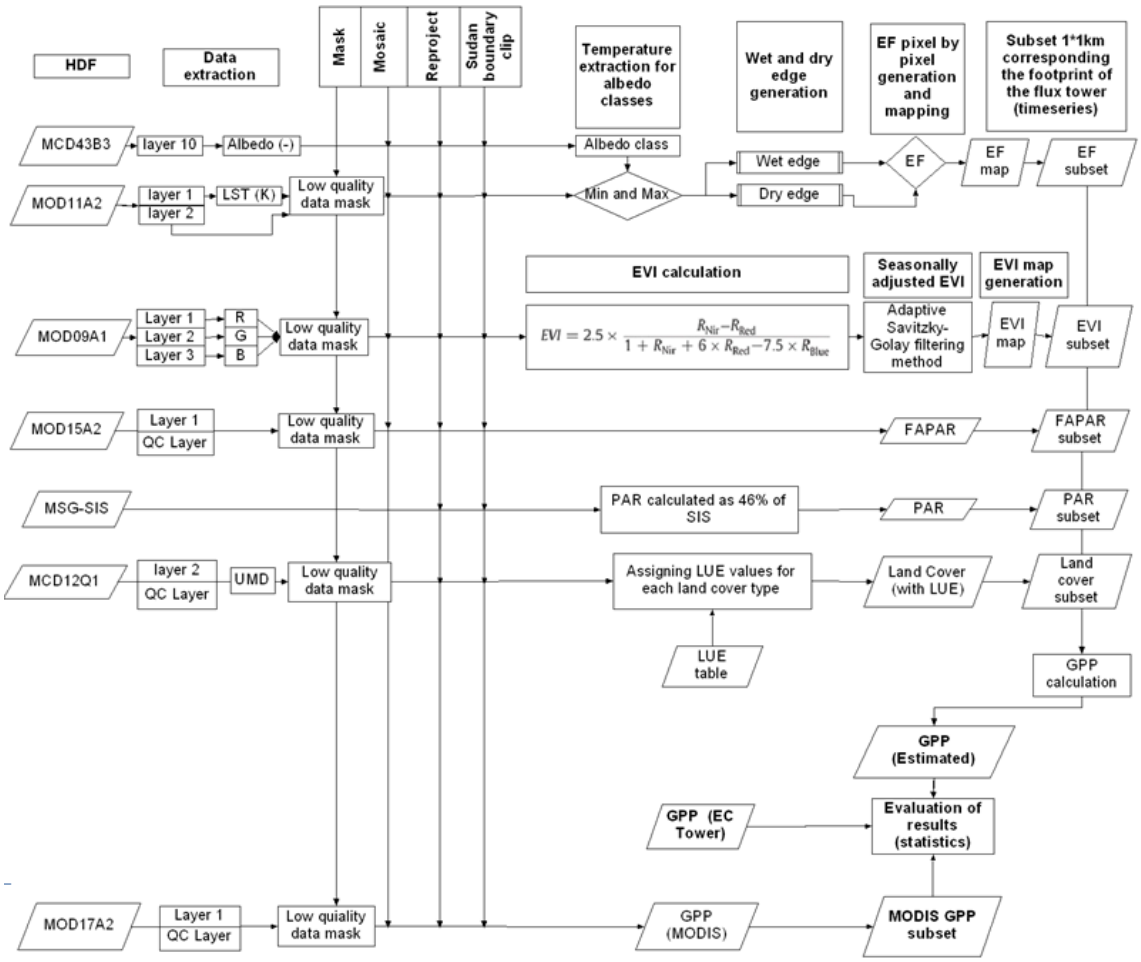

Figure 6. Process tree.

The pre- processing of data started with creation of mosaics from the tiles corresponding to the study area, followed by the extraction of the relevant layers for each product and the re-projection from Sinusoidal to WGS84 using the MODIS MRT tool (Processes & Active, 2010).

The values marked as low quality data (cloud contamination) or no data were masked out and excluded from the products MOD1A2, MOD09A1, MOD15A2 and MOD17A2H.

The values of the relevant layers were multiplied by their respective scaling factor to obtain the desired units as found in their respective MODIS products description site.
The evaporative fraction was calculated using the code provided by dr. Nutini and dr. Candiani taking as input mosaics of HDF files to produce EF maps for each MODIS date.

For EVI, the data corresponding to the area of interest, Demokeya tower, was obtained from Jonas Ardö (Ardö *et al*, 2016); being seasonally adjusted as previously explained. For country-scale calculations, the compilation of EVI time series was made from surface reflectance MOD09A1 bands 1, 2 and 3 but no further adjustments were made.
The outputs were clipped with a shape file to exclude the areas out of the territory of Sudan and ε max values from the designed LUT were assigned for their corresponding land cover classes of the MCD12Q1 product.
Small subsets corresponding EC tower footprint were extracted (for products at 500m resolution, 4 pixels to cover ~1Km^2; and for products at 1km resolution, 2 pixels to cover 2Km^2). Figure 7 shows the choice of pixels that were included.

Figure 7. EC tower Subset. Shows the selected pixels from the MODIS products that were considered to be equal as the EC tower footprint. Some products have 1km pixel size while others have 500 mts. The yellow point represents the position of the tower.

Since MODIS data is given as the average of the 8-days observations and MSG and EC are found daily, the MODIS values for the corresponding 8 days were kept constant.
There were gaps in the MSG-SIS data in the following dates and those were filled by averaging the values of the previous and subsequent dates. 6/9/2007, 3/12/2007 to 11/12/2007, 1/3/2007, 14/3/2007 to 18/3/2007, 1/12/2008 to 9/12/2008, 18/5/2009 to 22 /4 /2009, 15/8/2009 to 20/8/2009.

For the case of MODIS subsets, the missing values were obtained as an average of the neighboring pixels.

The two proposed formulas were calculated and plotted against EC tower measurements and the corresponding MODIS17A2 subset.

Results

The study tested two formulas to estimate GPP using evaporative fraction as a water stress factor. Figure 8 shows that MODIs MOD17A2 consistently underestimated GPP, followed by the formula using EF and EVI and the best estimation were obtained using the EF and FAPAR. Even though there is an underestimation during the rainy season for the three cases.

The maximum GPP recorded in Demokeya by the EC tower was 8.41 gC $m^{-2}d^{-1}$ (24-aug-2008). The maximum GPP estimated by the formula using FAPAR was 3.83 gC $m^{-2}d^{-1}$ (3-sept-2008) followed by 2.45 gC $m^{-2}d^{-1}$ (4-sep-2007) using EVI as surrogate of FAPAR. For the case of MODIS GPP the maximum value obtained was 1.89 gC $m^{-2}d^{-1}$ (23/aug/2007).

On average GPP estimated using FAPAR and EF accounted for 57.34% of the GPP estimated by the EC tower, followed by 40.42% when EVI and EF was used as surrogate of FAPAR. While MODIS17A2 only estimated the 23.95%

If the evaporative fraction coefficient was not included in the models the results would show an overestimation of values during the dry season but a better fit for the rainy season (figure 9). This suggests that a further adjustment to use of the EF would lead to better estimations.

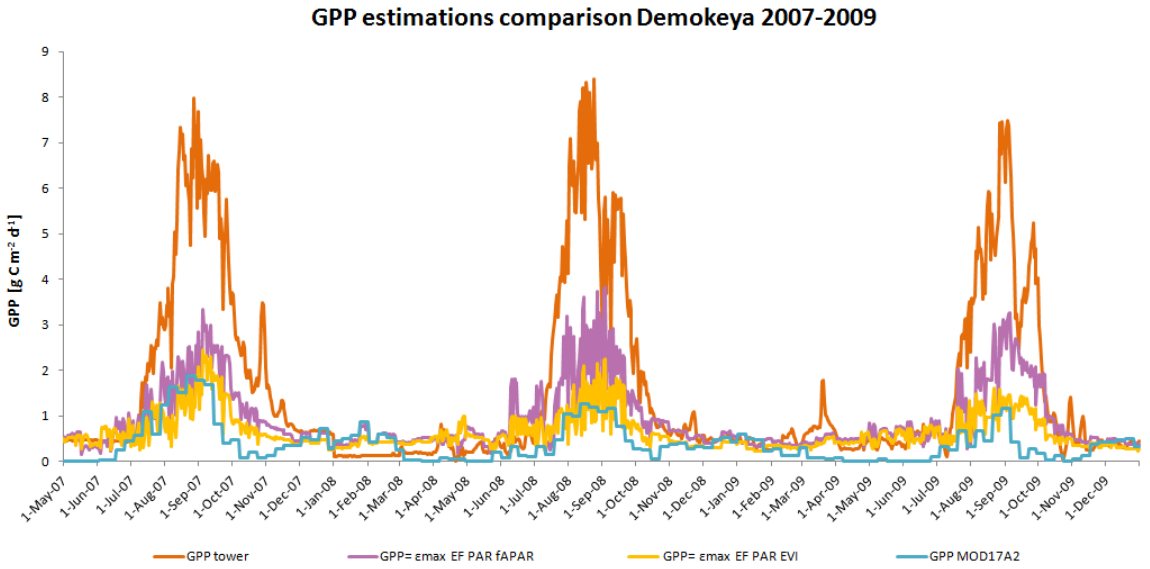

Figure 8. GPP estimations comparison. The graph compares the attained grams of carbon per square meter at each time step of the study period. In orange the GPP measured from the flux tower, purple and yellow for GPP estimated with the two models and blue for the values from MODIS GPP product.

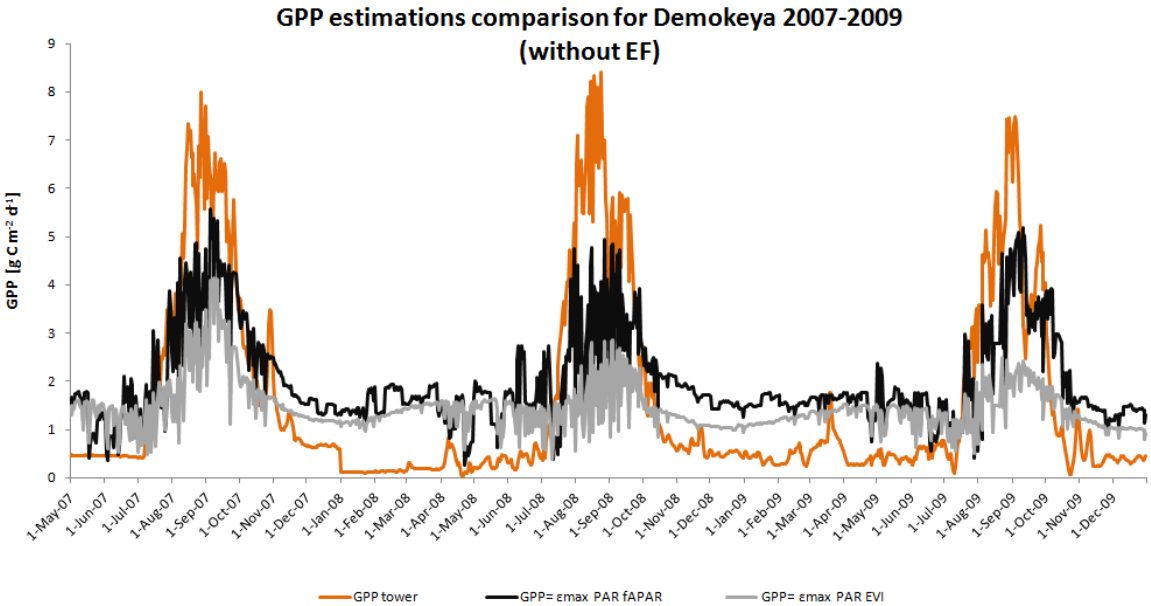

Figure 9. GPP estimation comparison (without EF). The graph compares the attained grams of carbon per square meter at each time step of the study period without including the evaporative fraction in any of the two models. If the evaporative fraction coefficient was not included in the models the results would show an overestimation of values during the dry season but a better fit for the rainy season (figure 9). This suggests that a further adjustment to use of the EF would lead to better estimations.

Scater plots

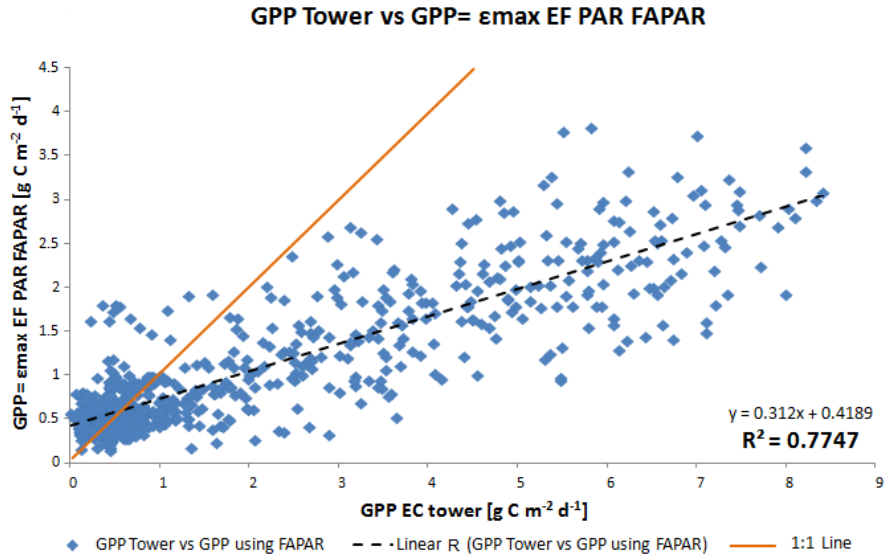

Figure 10. Scatter plot of GPP tower vs GPP = εMax EF PAR FAPAR. There is a good correlation for GPP values lower than 1 g C m^{-2} day^{-1} (dry season), but in higher GPP values (wet season) the correlation worsens considerably. Still, with a RMSE of 1.58, this is the model that performed the best among the 5 models tested.

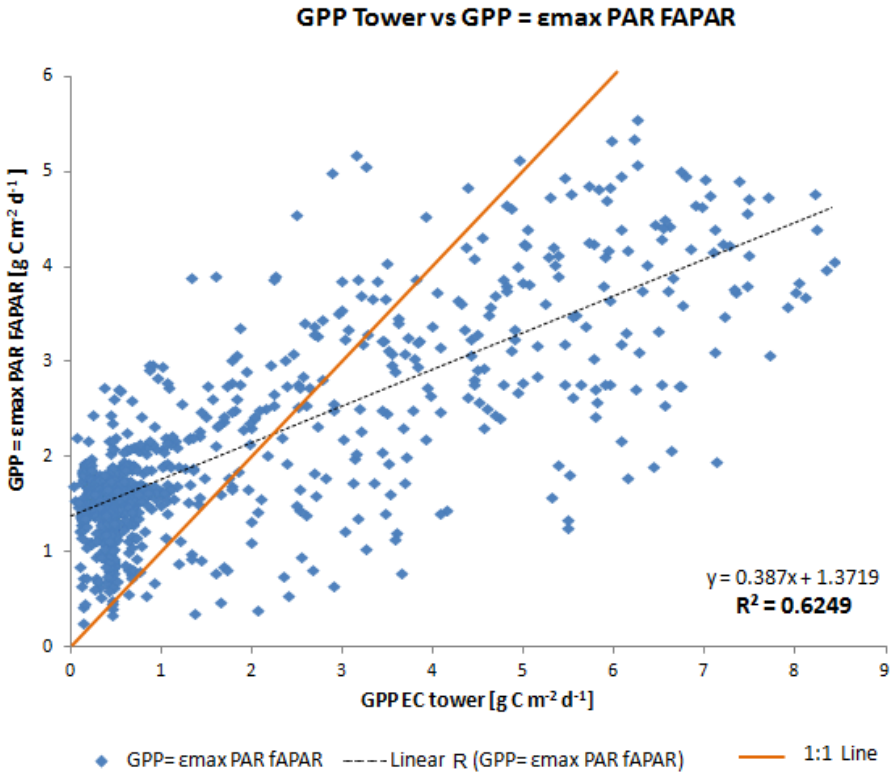

Figure 12. Scatter plot of GPP tower vs GPP = εMax PAR FAPAR. The exclusion of the EF from the model resulted in a shift towards higher GPP values. It decreased the correlation of low GPP values (dry season) but increased the correlation of high GPP values (wet season).

RMSE: 1.42.

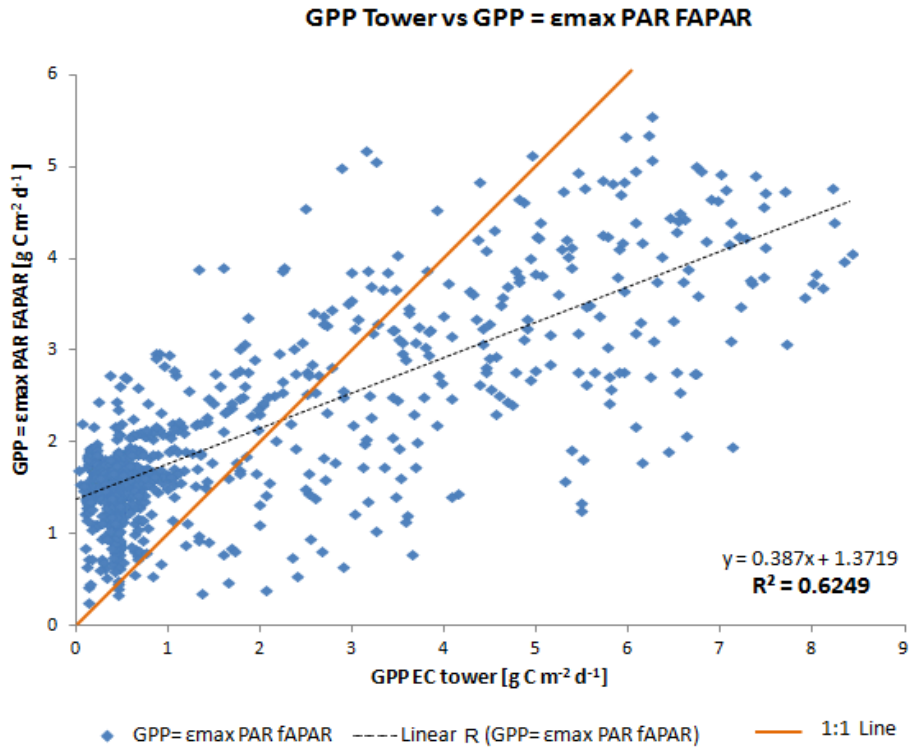

Figure 12. Scatter plot of GPP tower vs GPP = εMax PAR FAPAR. The exclusion of the EF from the model resulted in a shift towards higher GPP values. It decreased the correlation of low GPP values (dry season) but increased the correlation of high GPP values (wet season). RMSE: 1.42.

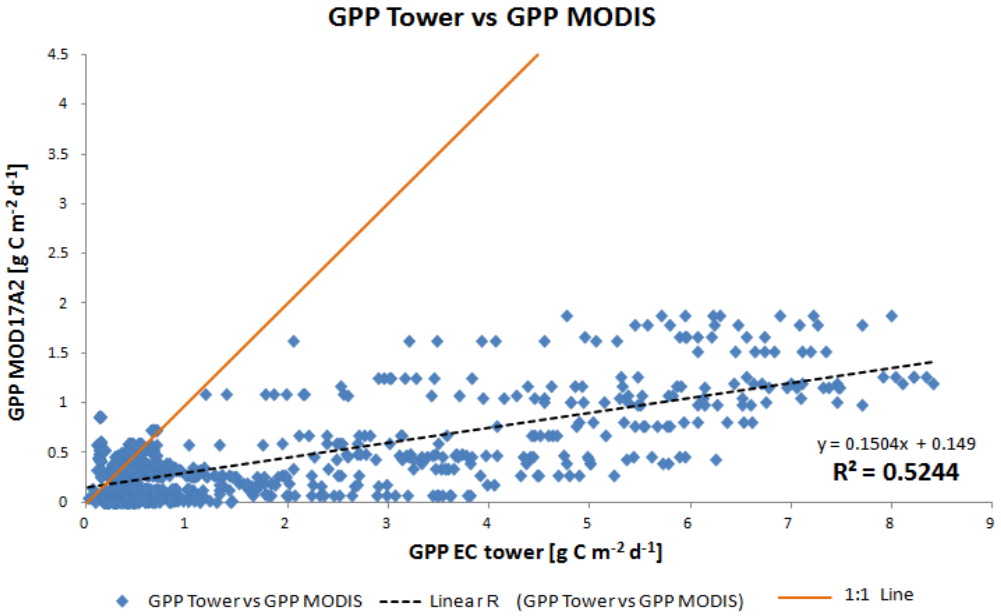

Figure 13. Scatter plot of GPP tower vs MODIS GPP. There is a very good correlation for very low values (dry season) but at higher values (wet season) the correlation is very poor. RMSE: 2.11.

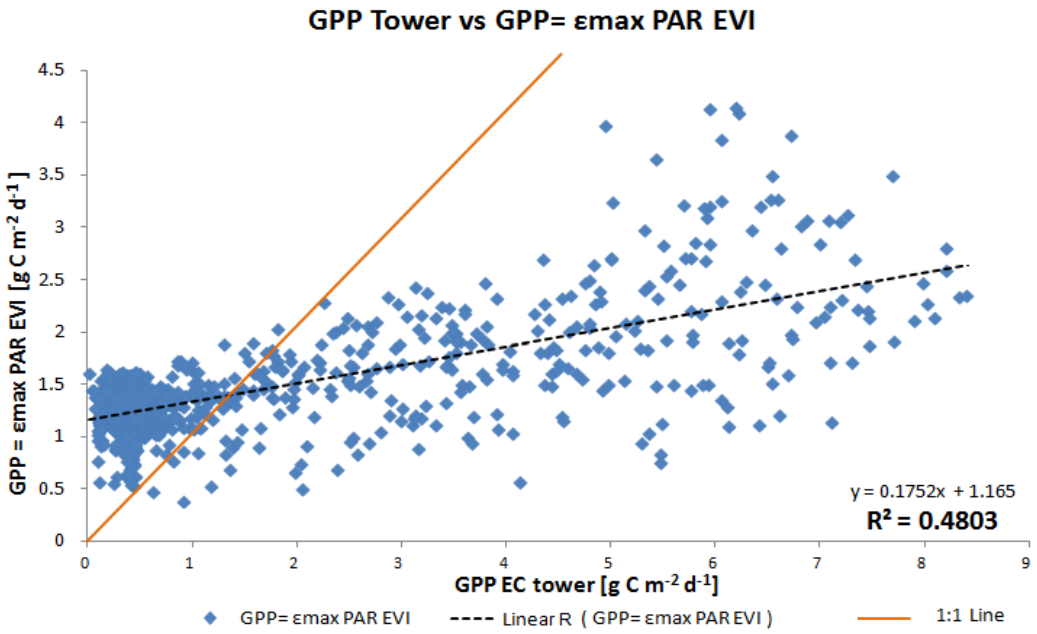

Figure 14. Scatter plot of GPP tower vs GPP = εMax PAR EVI. The exclusion of the EF from the model resulted in a shift towards higher GPP values with a very poor correlation for low GPP values (dry season). RMSE: 1.70.

Results summary

Table 4 shows the comparison of the annual results obtained from the different GPP models against the EC flux tower estimations. The first gray row shows the annual GPP accumulation in the 1Km^2 corresponding to the EC flux tower's footprint of Demokeya site. The second gray row shows the fraction obtained dividing the calculated GPP by the tower estimates.

Table 4. Annual GPP comparison

	2007*		2008		2009	
	g C m^{-2}y^{-1}	Fraction of tower estimation	g C m^{-2}y^{-1}	Fraction of tower estimation	g C m^{-2}y^{-1}	Fraction of tower estimation
GPP EC flux tower	547.31	-	529.18	-	489.15	-
GPP = εmax • EF • PAR • FAPAR	260.17	0.475	334.23	0.632	303.35	0.426
GPP = εmax • EF • PAR • EVI	192.59	0.352	232.05	0.439	208.20	0.620
PP = εmax • PAR • FAPAR	554.66	1.013	698.43	1.32	691.65	1.003
GPP MOD17A2	142.50	0.260	140.79	0.266	91.71	0.188
GPP = εmax • PAR • EVI	414.35	0.757	506.28	0.957	490.63	1.003

*Includes only the months from May to December 2007

Table 5 shows the comparison of results obtained from the different GPP models against the EC flux tower for the entire period. The first row displays the accumulated GPP, the second row shows the fraction obtained dividing the calculated GPP by the tower estimates, the third and fourth rows represent the coefficient of determination and root mean squared error respectively.

Table 5. Comparison of estimated GPP for study period, R^2 and RMSE.

	g C m^{-2} study $period^{-1}$	Fraction of tower estimation	R^2	RMSE g C m^{-2} day^{-1}
GPP TOWER	1565.63	-	-	-
GPP = εmax • EF • PAR • FAPAR	897.75	0.573	0.77	1.58
GPP = εmax • EF • PAR • EVI	632.85	0.404	0.71	1.94
PP = εmax • PAR • FAPAR	1944.75	1.242	0.62	1.42
GPP MOD17A2	375.00	0.234	0.52	2.11
GPP = εmax • PAR • EVI	1411.26	0.901	0.48	1.70

Observing the R^2 and the RMSE from the tables 4 and 5 and Figures 10 to 14, the closest estimates are obtained from the model: **GPP = εmax * (EF)** * **PAR *FAPAR**.

Discussion

The use of the evaporative fraction as a limiting factor in a LUE model has proven to increase the accuracy of the GPP estimations during the dry seasons, but at the same time increasing the underestimation during the rainy seasons. The accuracy of the study can only be tested against the EC flux tower in Sudan (Demokeya site) since is the only available tower in the country. Therefore additional flux towers would provide more ground measurements in order to test the performance of the models under different land cover types.

Some of the discrepancies between the GPPEC and modeled GPP values might be caused due to issues from the remote sensing products such as frequent cloud cover in the wet season, the atmospheric influences (Kaufman et al., 1992), geolocation accuracy (Hashimoto et al., 2012), radiative contribution from the background especially in sparsely vegetated areas (Tian et al., 2000), differences in spatial and temporal resolution and maximum value compositing of some MODIS products (Sjöström et al., 2011). Additionally, EC tower measurements can present biases in the eddy covariance technique, Carvalhais, et al., (2009) explained that the standard approach for extrapolating night-time Reco does not consider the reduction in leaf respiration in day time in comparison to night time, leading to a possible overestimations of Reco and GPP. Other source of discrepancy may be also due to delays of greening productivity as a response to wetting (Fensholt,et al., ;Williams et al., 2009)

Complementing the measurements of the tower with studies of dry matter samples would provide additional data to obtain better representation of reality.

Several studies have previously used EF as an indicator of water availability since water is a limiting factor for vegetation in semi arid areas. However, Gentine et al.,(2007) states that sensible heat flux is generally high in areas with low LAI, as LAI increases, sensible

heath flux can become negative. This effect causes EF to exceed unity in areas with high soil moisture conditions and high LAI.
Other options exist for calculating factors that limit photosynthesis in water-scarce conditions. For example, the ratio of actual evapotranspiration (AET) to potential (PET) is linearly related to water stress at semi arid perennial grasslands (Nouvellon et al 2000). Also, (Garbulsky et al., 2010) in their study concluded that the performance of the ratio AET/PET was better than EF over savanna ecosystems when determining the Radiation Use Efficiency.
Promising approaches to improve GPP estimations have been explored. Kanniah, et al., (2010) obtained results of only 6% error compared to GPP from EC tower, carrying out an analysis based in vegetation maps in terms of spatial and temporal patterns of vegetation, classified in accordance to structural characteristics such as height and foliage projective cover, broad vegetation groups and spatial extent.
Further research needs to be carried out and additional control points (EC towers) would be needed to be able to assess the accuracy of the models for the other land cover classes found in the study area.

Conclusions

The use of EF increases the accuracy of the GPP estimations during the dry seasons but increases the underestimation during the rainy seasons.

The use of FAPAR in the LUE model derived more accurate estimations than using EVI for the $1km^2$ subset of the study area.

In general the two models performed significantly better compared to the MOD17A2 MODIS GPP product.

Acknowledgements

I express my deepest gratitude to the National Council of Science and Technology of Mexico (CONACYT) for their financial support for the realization of my master's studies.

References

Abdi, A. M., Seaquist, J., Tenenbaum, D. E., Eklundh, L., & Ardö, J. (2014). The supply and demand of net primary production in the Sahel. *Environmental Research Letters*, *9*(9), 094003. doi:10.1088/1748-9326/9/9/094003

Acker, R. H., Kammen, D. M., Almeida, M. P., Perpiñán, O., Narvarte, L., Antonanzas-Torres, F., … Hinssen, Y. B. L. (2010). EUMETSAT Satellite Application Facility on Climate Monitoring CM SAF Cloud , Albedo , Radiation dataset , Surface Albedo Product User Manual. *Solar Energy*, *35*(1), 1–24. doi:10.5676/EUM

Aminou, D. M. A. (2002). MSG 's SEVIRI Instrument. *ESA Bulletin*, 15–17.

Ardö, J. (2013). A 10-Year dataset of basic meteorology and soil properties in Central Sudan. *Dataset Papers in Geosciences*, *2013*, 1–6. doi:10.7167/2013/297973

Baret, F., Bacour, C., Béal, D., Weiss, M., Berthelot, B., & Regner, P. (2006). Algorithm Theoretical Basis Document for MERIS Top of Canopy Land Products (TOC _ VEG). *Contract*, (March), 1–25.

Beer, Reichstein, C., Rödenbeck, Arain, A., & Baldocchi. (2010). Terrestrial Gross Carbon Dioxide Uptake: Global Distribution and Covariation with Climate, *329*(August), 834–839.

Bondeau, A Cramer, W., Kicklighter, D. W., Moore, B., Churkina, G., Nemry, B., Ruimy, A., & Schloss, a L. (1999). Comparing global models of terrestrial net primary productivity (NPP): overview and key results. *Global Change Biology*, *5*(1), 1–15. doi:10.1046/j.1365-2486.1999.00001.x

Carter, G. a, & Knapp, a K. (2001). Leaf optical properties in higher plants: linking spectral characteristics to stress and chlorophyll concentration. *American Journal of Botany*, *88*(4), 677–684. doi:10.2307/2657068

Carvalhais, N., Reichstein, M., Jung, M., Lasslop, G., & Papale, D. (2009). Considerations on eddy-covariance data from FLUXNET in model-data fusion and data-assimilation Principles of eddy-covariance measurements, (November), 9–12.

Eklundh, L., & Olsson, L. (2003). Vegetation index trends for the African Sahel 1982–1999. *Geophys. Res. Lett.*, *30*(8), 1430. doi:10.1029/2002GL016772

European Fluxes Database Cluster - Sites List. (n.d.). Retrieved May 25, 2016, from http://gaia.agraria.unitus.it/home/sites-list

Fallis, A. . (2013). User Guide for the MODIS Land Cover Type Product (MCD12Q1). *Journal of Chemical Information and Modeling*, *53*(9), 1689–1699. doi:10.1017/CBO9781107415324.004

Fensholt, R., Huber, S., Proud, S. R., & Mbow, C. (2010). Infrared Reflectance Data From Polar Orbiting and Geostationary Platforms. *IEEE Journal of Selected Topics in Applied Earth Observations and Remote Sensing*, *3*(3), 271–285.

Galleguillos, M., Jacob, F., Pr??vot, L., French, A., & Lagacherie, P. (2011). Comparison of two temperature differencing methods to estimate daily evapotranspiration over a Mediterranean vineyard watershed from ASTER data. *Remote Sensing of Environment*, *115*(6), 1326–1340. doi:10.1016/j.rse.2011.01.013

Garbulsky, M. F., Peñuelas, J., Papale, D., Ardö, J., Goulden, M. L., Kiely, G., … Filella, I. (2010). Patterns and controls of the variability of radiation use efficiency and primary productivity across terrestrial ecosystems. *Global Ecology and Biogeography*, *19*(2), 253–267. doi:10.1111/j.1466-8238.2009.00504.x

Garbulsky, M. F., Peñuelas, J., Papale, D., & Filella, I. (2008). Remote estimation of carbon dioxide uptake by a Mediterranean forest. *Global Change Biology*, *14*(12), 2860–2867. doi:10.1111/j.1365-2486.2008.01684.x

Gentine, P., Entekhabi, D., Chehbouni, A., Boulet, G., & Duchemin, B. (2007). Analysis of evaporative fraction diurnal behaviour. *Agricultural and Forest Meteorology*, *143*(1-2), 13–29. doi:10.1016/j.agrformet.2006.11.002

Gitelson, A. A., Vi??a, A., Verma, S. B., Rundquist, D. C., Arkebauer, T. J., Keydan, G., … Suyker, A. E. (2006). Relationship between gross primary production and chlorophyll content in crops: Implications for the synoptic monitoring of vegetation productivity. *Journal of Geophysical Research Atmospheres*, *111*(8), 1–13. doi:10.1029/2005JD006017

Gobron, N., & Verstraete, M. M. (2009). Fraction of Absorbed Photosynthetically Active Radiation (FAPAR). *Assessment of the Status of the Development of the Standards for the Terrestrial Essential Climate Variables*, (T10-fAPAR), 24. Retrieved from http://www.fao.org/gtos/ECV-T10.html

Gower, S. T., Kucharik, C. J., & Norman, J. M. (1999). Direct and indirect estimation of leaf area index, f(APAR), and net primary production of terrestrial ecosystems. *Remote Sensing of Environment*, *70*(1), 29–51. doi:10.1016/S0034-4257(99)00056-5

Granger, R. J. (2000). Satellite-derived estimates of evapotranspiration in the Gediz basin. *Journal of Hydrology*, *229*(1-2), 70–76. doi:10.1016/S0022-1694(99)00200-0

Hashimoto, H., Dungan, J. L., White, M. A., Yang, F., Michaelis, A. R., Running, S. W., & Nemani, R. R. (2008). Satellite-based estimation of surface vapor pressure deficits using MODIS land surface temperature data. *Remote Sensing of Environment*, *112*(1), 142–155. doi:10.1016/j.rse.2007.04.016

Hashimoto, H., Wang, W., Milesi, C., White, M. A., Ganguly, S., Gamo, M., … Nemani, R. R. (2012). Exploring simple algorithms for estimating gross primary production in forested areas from satellite data. *Remote Sensing*, *4*(1), 303–326. doi:10.3390/rs4010303

Hein, L., De Ridder, N., Hiernaux, P., Leemans, R., De Wit, A., & Schaepman, M. (2011). Desertification in the Sahel: Towards better accounting for ecosystem dynamics in the interpretation of remote sensing images. *Journal of Arid Environments*, *75*(11), 1164–1172. doi:10.1016/j.jaridenv.2011.05.002

Hendry, B. Y. G. a F., Houghton, J. D., Brown, S. B., & Sio, S. (1987). TANSLEY REVIEW NO . 11 THE DEGRADATION OF CHLOROPHYLL — A BIOLOGICAL ENIGMA ' Unit of Comparative Plant Ecology (NERC), Department of Botany , The 1 . The phenomenon of chlorophyll breakdown biochemical processes . Its biosynthesis determines the charac. *New Phytologist*, *0*(11), 255–302.

Huete, A., Didan, K., Miura, T., Rodriguez, E. P., Gao, X., & Ferreira, L. G. (2002). Overview of the radiometric and biophysical performance of the MODIS vegetation indices. *Remote Sensing of Environment*, *83*(1-2), 195–213. doi:10.1016/S0034-4257(02)00096-2

Huete, A. R., Liu, H. Q., Batchily, K., & Van Leeuwen, W. (1997). A comparison of vegetation indices over a global set of TM images for EOS-MODIS. *Remote Sensing of Environment*, *59*(3), 440–451. doi:10.1016/S0034-4257(96)00112-5

Iqbal, M. (1983). An Introduction to Solar Radiation. *Orlando: Academic Press.*

Jönsson, P., & Eklundh, L. (2002). Seasonality extraction by function fitting to time-series of satellite sensor data. *IEEE Transactions on Geoscience and Remote Sensing*, *40*(8), 1824–1832. doi:10.1109/TGRS.2002.802519

Kanniah, K. D., Beringer, J., Hutley, L. B., Tapper, N. J., & Zhu, X. (2009). Evaluation of Collections 4 and 5 of the MODIS Gross Primary Productivity product and algorithm improvement at a tropical savanna site in northern Australia. *Remote Sensing of Environment*, *113*(9), 1808–1822. doi:10.1016/j.rse.2009.04.013

Kanniah, J. Beringer, L. H. (2010). Analysis of the spatial and temporal variability of savanna productivity in the Northern Territory, Australia using MODIS data. *International Archives of the Photogrammetry, Remote Sensing and Spatial Information Science*, *38*. doi:10.1017/CBO9781107415324.004

Kaufman, Y. J., Tanré, D., Markham, B., & Gitelson, A. A. (1992). Atmospheric Effects on the NDVI--Strategies for Its Removal. doi:10.1109/IGARSS.1992.578402.

Krofcheck, D., Eitel, J., Lippitt, C., Vierling, L., Schulthess, U., & Litvak, M. (2015). Remote Sensing Based Simple Models of GPP in Both Disturbed and Undisturbed Piñon-Juniper Woodlands in the Southwestern U.S. *Remote Sensing*, *8*(1), 20. doi:10.3390/rs8010020

Kurc, S. A., & Small, E. E. (2004). Dynamics of evapotranspiration in semiarid grassland and shrubland ecosystems during the summer monsoon season, central New Mexico. *Water Resources Research*, *40*(9), 1–15. doi:10.1029/2004WR003068

Landsberg, J. J., & Waring, R. H. (1997). A generalised model of forest productivity using simplified concepts of radiation-use efficiency, carbon balance and partitioning. *Forest Ecology and Management*, *95*(3), 209–228. doi:10.1016/S0378-1127(97)00026-1

Li, S. G., Eugster, W., Asanuma, J., Kotani, A., Davaa, G., Oyunbaatar, D., & Sugita, M. (2006). Energy partitioning and its biophysical controls above a grazing steppe in central Mongolia. *Agricultural and Forest Meteorology*, *137*(1-2), 89–106. doi:10.1016/j.agrformet.2006.03.010

Li, X., & Strahler, A. (1985). Geometric-optimal modeling of a conifer forest canopy. *IEEE Transactions on Geoscience and Remote Sensing*, *23*(5), 705–721.

Ma, X., Huete, A., Yu, Q., Restrepo-Coupe, N., Beringer, J., Hutley, L. B., … Eamus, D. (2014). Parameterization of an ecosystem light-use-efficiency model for predicting savanna GPP using MODIS EVI. *Remote Sensing of Environment*, *154*(1), 253–271. doi:10.1016/j.rse.2014.08.025

MÄKELÄ, A., PULKKINEN, M., KOLARI, P., LAGERGREN, F., BERBIGIER, P., LINDROTH, A., … HARI, P. (2007). Developing an empirical model of stand GPP with the LUE approach: analysis of eddy covariance data at five contrasting conifer sites in Europe. *Global Change Biology*, 071124112207003–??? doi:10.1111/j.1365-2486.2007.01463.x

McCree, K. J. (1981). Physiological Plant Ecology I: Responses to the Physical Environment. In O. L. Lange, P. S. Nobel, C. B. Osmond, & H. Ziegler (Eds.), (pp. 41–55). Berlin, Heidelberg: Springer Berlin Heidelberg. doi:10.1007/978-3-642-68090-8_3

Merbold, L., Ardö, J., Arneth, a., Scholes, R. J., Nouvellon, Y., de Grandcourt, a., … Kutsch, W. L. (2008). Precipitation as driver of carbon fluxes in 11 African ecosystems. *Biogeosciences Discussions*, *5*(5), 4071–4105. doi:10.5194/bgd-5-4071-

2008
Metz, H. C. (GPO for the L. of C. (1991). Sudan - Geography. Retrieved March 16, 2016, from http://countrystudies.us/sudan/33.htm
Monteith, J. L. (1972). Solar radition and productivity in tropical ecosystems. *Journal Of Applied Ecology*. doi:10.2307/2401901
Myneni, R. B., Knyazikhin, Y., Privette, J. L., Running, S. W., Nemani, R., Zhang, Y., … Votava, P. (1999). MODIS Leaf Area Index (LAI) And Fraction Of Photosynthetically Active Radiation Absorbed By Vegetation (FPAR) Product. *Modis Atbd, Version 4.*, 130. doi:http://eospso.gsfc.nasa.gov/atbd/modistables.html
Myneni, R. B., & Williams, D. L. (1994). On the relationship between FAPAR and NDVI. *Remote Sensing of Environment*, *49*(3), 200–211. doi:10.1016/0034-4257(94)90016-7
Nouvellon, Y., Seen, D. Lo, Rambal, S., B??gu??, A., Moran, M. S., Kerr, Y., & Qi, J. (2000). Time course of radiation use efficiency in a shortgrass ecosystem: Consequences for remotely sensed estimation of primary production. *Remote Sensing of Environment*, *71*(1), 43–55. doi:10.1016/S0034-4257(99)00063-2
Nutini, F., Boschetti, M., Candiani, G., Bocchi, S., & Brivio, P. A. (2014). Evaporative fraction as an indicator of moisture condition and water stress status in semi-arid rangeland ecosystems. *Remote Sensing*, *6*(7), 6300–6323. doi:10.3390/rs6076300
Ollinger, S. V, Richardson, A. D., Martin, M. E., Hollinger, D. Y., Frolking, S. E., Reich, P. B., … Schmid, H. P. (2008). Canopy nitrogen, carbon assimilation, and albedo in temperate and boreal forests: Functional relations and potential climate feedbacks. *Proceedings of the National Academy of Sciences of the United States of America*, *105*(49), 19336–41. doi:10.1073/pnas.0810021105
Olofsson, P., Lagergren, F., Lindroth, A., Lindstrom, J., Klemedtsson, L., Kutsch, W., & Eklundh, L. (2008). Towards operational remote sensing of forest carbon balance across Northern Europe. *Biogeosciences*, *5*(3), 817–832. doi:10.5194/bg-5-817-2008
Papale, D., Reichstein, M., Aubinet, M., Canfora, E., Bernhofer, C., Kutsch, W., … Yakir, D. (2006). Towards a standardized processing of Net Ecosystem Exchange measured with eddy covariance technique: algorithms and uncertainty estimation. *Biogeosciences*, *3*(4), 571–583. doi:10.5194/bg-3-571-2006
Peres, L. (2005). Land-surface emissivity maps based on MSG/SEVIRI information. *Eumetsat.Int*, 1–8. Retrieved from http://www.eumetsat.int/groups/cps/documents/document/pdf_conf_p46_s4_03_peres_v.pdf
Potter, C. S., Klooster, S., & Brooks, V. (1999). Interannual Variability in Terrestrial Net Primary Production: Exploration of Trends and Controls on Regional to Global Scales. *Ecosystems*, *2*(1), 36–48. doi:10.1007/s100219900056
PRINCE, S. D. (1991). A model of regional primary production for use with coarse resolution satellite data. *International Journal of Remote Sensing*, *12*(6), 1313–1330. doi:10.1080/01431169108929728
Processes, L., & Active, D. (2010). MODIS Reprojection Tool Swath User Manual. *Processing*, (December), 1–49.
Reichstein, M., Falge, E., Baldocchi, D., Papale, D., Aubinet, M., Berbigier, P., … Valentini, R. (2005). On the separation of net ecosystem exchange into assimilation and ecosystem respiration: Review and improved algorithm. *Global Change*

Biology, *11*(9), 1424–1439. doi:10.1111/j.1365-2486.2005.001002.x

Rossini, M., Cogliati, S., Meroni, M., Migliavacca, M., Galvagno, M., Busetto, L., … Colombo, R. (2012). Remote sensing-based estimation of gross primary production in a subalpine grassland. *Biogeosciences*, *9*(7), 2565–2584. doi:10.5194/bg-9-2565-2012

Ruimy, A., Saugier, B., & Dedieu, G. (1994). Methodology for the estimation of terrestrial net primary production from remotely sensed data. *Journal of Geophysical Research*, *99*(D3), 5263. doi:10.1029/93JD03221

RUNNING, S. W., NEMANI, R. R., HEINSCH, F. A., ZHAO, M., REEVES, M., & HASHIMOTO, H. (2004). A Continuous Satellite-Derived Measure of Global Terrestrial Primary Production. *BioScience*, *54*(6), 547. doi:10.1641/0006-3568(2004)054[0547:ACSMOG]2.0.CO;2

Running, S. W., & Zhao, M. (2015). User's Guide, Daily GPP and Annual NPP (MOD17A2/A3) Products NASA Earth Observing System MODIS Land Algorithm, 28.

Russell, G., Jarvis, P. G., & Monteith, J. L. (1989). Absorption of Radiation by Canopies and Stand Growth. *Plant Canopies : Their Growth, Form and Function*, *31*, 21–39.

Sims, D. A., Rahman, A. F., Cordova, V. D., El-Masri, B. Z., Baldocchi, D. D., Bolstad, P. V., … Xu, L. (2008). A new model of gross primary productivity for North American ecosystems based solely on the enhanced vegetation index and land surface temperature from MODIS. *Remote Sensing of Environment*, *112*(4), 1633–1646. doi:10.1016/j.rse.2007.08.004

Sjöström, M., Ardö, J., Arneth, A., Boulain, N., Cappelaere, B., Eklundh, L., … Veenendaal, E. M. (2011a). Exploring the potential of MODIS EVI for modeling gross primary production across African ecosystems. *Remote Sensing of Environment*, *115*(4), 1081–1089. doi:10.1016/j.rse.2010.12.013

Sjöström, M., Ard??, J., Arneth, A., Boulain, N., Cappelaere, B., Eklundh, L., … Veenendaal, E. M. (2011b). Exploring the potential of MODIS EVI for modeling gross primary production across African ecosystems. *Remote Sensing of Environment*, *115*(4), 1081–1089. doi:10.1016/j.rse.2010.12.013

Sjöström, M., Ardö, J., Eklundh, L., El-Tahir, B. a., El-Khidir, H. a. M., Pilesjö, P., & Seaquist, J. (2008). Evaluation of satellite based indices for primary production estimates in a sparse savanna in the Sudan. *Biogeosciences Discussions*, *5*(4), 2985–3011. doi:10.5194/bgd-5-2985-2008

Stagakis, S., Markos, N., Levizou, E., & Kyparissis, A. (2007). Forest Ecosystem Dynamics Using Spot and Modis Satellite Images. *Office*, *2007*(April).

Strahler, A. H., & Muller, J. P. (1999). MODIS BRDF Albedo Product : Algorithm Theoretical Basis Document. *MODIS Product ID: MOD43*, *Version 5*.(April), 1–53. Retrieved from \Biblioteca_Digital_SPR\Strahler1999_ATBD.pdf

Tian, Y., Zhang, Y., Knyazikhin, Y., Myneni, R. B., Glassy, J. M., Dedieu, G., & Running, S. W. (2000). Prototyping of MODIS LAI and FPAR algorithm with LASUR and LANDSAT data. *IEEE Transactions on Geoscience and Remote Sensing*, *38*(5 II), 2387–2401. doi:10.1109/36.868894

Tucker, C. J. (1979). Red and photographic infrared linear combinations for monitoring vegetation. *Remote Sensing of Environment*, *8*(2), 127–150. doi:10.1016/0034-4257(79)90013-0

Turner, D. P., Urbanski, S., Bremer, D., Wofsy, S. C., Meyers, T., Gower, S. T., & Gregory, M. (2003). A cross-biome comparison of daily light use effciency for gross primary production. *Global Change Biology*, *9*, 383–395.

Vermote, E. F. (2011). MODIS Surface Reflectance User ' s Guide. *Orbit An International Journal On Orbital Disorders And Facial Reconstructive Surgery*, 1–40.

Wan, Z. (2006). MODIS Land Surface Temperature Products Users ' Guide, (September), 30.

Wang, S., & Mo, X. (2015). Comparison of multiple models for estimating gross primary production using remote sensing data and fluxnet observations. *Proceedings of the International Association of Hydrological Sciences*, *368*(August 2014), 75–80. doi:10.5194/piahs-368-75-2015

Williams, C. A., Hanan, N., Scholes, R. J., & Kutsch, W. (2009). Complexity in water and carbon dioxide fluxes following rain pulses in an African savanna. *Oecologia*, *161*(3), 469–480. doi:10.1007/s00442-009-1405-y

Yuan, W., Liu, S., Zhou, G., Zhou, G., Tieszen, L. L., Baldocchi, D., … Wofsy, S. C. (2007). Deriving a light use efficiency model from eddy covariance flux data for predicting daily gross primary production across biomes. *Agricultural and Forest Meteorology*, *143*(3-4), 189–207. doi:10.1016/j.agrformet.2006.12.001

Personal communication

The IDL code to calculate the Evaporative Fraction was kindly provided by Francesco Nutini and Gabriele Candiani, Institute of Electromagnetic Sensing of Environment, National Research Council of Italy (CNR-IREA), Via Bassini 15, Milan 20133, Italy.

Department of Physical Geography and Ecosystem Science, Lund University

Lund University GEM thesis series are master theses written by students of the international master program on Geo-information Science and Earth Observation for Environmental Modelling and Management (GEM). The program is a cooperation of EU universities in Iceland, the Netherlands, Poland, Sweden and UK, as well a partner university in Australia. In this series only master thesis are included of students that performed their project at Lund University. Other theses of this program are available from the ITC, the Netherlands (www.gem-msc.org or www.itc.nl).

The student thesis reports are available at the Geo-Library, Department of Physical Geography and Ecosystem Science, University of Lund, Sölvegatan 12, S-223 62 Lund, Sweden. Report series started 2013. The complete list and electronic versions are also electronic available at the LUP student papers (https://lup.lub.lu.se/student-papers/search/) and through the Geo-library (www.geobib.lu.se).

1 Soheila Youneszadeh Jalili (2013) The effect of land use on land surface temperature in the Netherlands
2 Oskar Löfgren (2013) Using Worldview-2 satellite imagery to detect indicators of high species diversity in grasslands
3 Yang Zhou (2013) Inter-annual memory effects between Soil Moisture and NDVI in the Sahel
4 Efren Lopez Blanco (2014) Assessing the potential of embedding vegetation dynamics into a fire behaviour model: LPJ-GUESS-FARSITE
5 Anna Movsisyan (2014) Climate change impact on water and temperature conditions of forest soils: A case study related to the Swedish forestry sector
6 Liliana Carolina Castillo Villamor (2015) Technical assessment of GeoSUR and comparison with INSPIRE experience in the context of an environmental vulnerability analysis using GeoSUR data
7 Hossein Maazallahi (2015) Switching to the "Golden Age of Natural Gas" with a Focus on Shale Gas Exploitation: A Possible Bridge to Mitigate Climate Change?
8 Mohan Dev Joshi (2015) Impacts of Climate Change on *Abies spectabilis*: An approach integrating Maxent Model (MAXent) and Dynamic Vegetation Model (LPJ-GUESS)
9 Altaaf Mechiche-Alami (2015) Modelling future wheat yields in Spain with LPJ-GUESS and assessing the impacts of earlier planting dates
10 Koffi Unwana Saturday (2015) Petroleum activities, wetland utilization and livelihood changes in Southern Akwa Ibom State, Nigeria: 2003-2015
11 José Ignacio Díaz González (2016) Multi-objective optimisation algorithms for GIS-based multi-criteria decision analysis: an application for evacuation planning
12 Gunjan Sharma (2016) Land surface phenology as an indicator of performance of conservation policies like Natura2000
13 Chao Yang (2016) A Comparison of Four Methods of Diseases Mapping
14 Xinyi Dai (2016) Dam site selection using an integrated method of AHP and GIS for decision making support in Bortala, Northwest China
15 Jialong Duanmu (2016) A multi-scale based method for estimating coniferous

forest aboveground biomass using low density airborne LiDAR data

16 Tanyaradzwa J. N. Muswera (2016) Modelling maize (Zea Mays L.) phenology using seasonal climate forecasts

17 Maria Angela Dissegna (2016) Improvement of the GPP estimations for Sudan using the evaporative fraction as water stress factor